

DEVELOPMENT OF THE AGGREGATE GRADATION MODELS USING DILATANCY PROPERTIES FOR RUTTING ASSESSMENT

Iman HARYANTO¹ and Osamu TAKAHASHI²

¹Graduate Student, Materials Science, Nagaoka University of Technology
(1603-1 Kamitomiokamachi, Nagaoka, Niigata, Japan)

E-mail: hary@stn.nagaokaut.ac.jp,

² Member of JSCE, Associate Professor, Dept. Civil and Environment Eng., Nagaoka University of Technology

Interaction of aggregate particles within hot mixture asphalt (HMA) mixtures provides shearing resistance. Configuration of the aggregate particles was spatially depicted as sphere assembly. Four types of aggregates gradation, namely stone matrix asphalt stone skeleton, coarse graded stone-sand skeleton, coarse graded and fine graded sand-stone skeleton were studied. The structure models of aggregate gradation were examined using dilatancy properties. Dilatancy tendencies of the spheres assembly models statistically agreed with the dilatancy properties measured from compression test. Simple doublet mechanistic qualitatively depicted the deformation tendencies of sphere models under wheel-tracking test.

Key Words: aggregate gradation, shear, sphere assembly, dilatancy, compression

1. INTRODUCTION

Aggregate gradation is one of main factors to characterize a performance of hot mix asphalt (HMA) mixtures. In fact, aggregate gradation is optimized to obtain the mixtures having sufficient resistances of rutting, durability and/or fracture^{1,2,3}. Asphalt researchers often categorize aggregate gradation of HMA mixtures using type of aggregate skeleton. Aggregate skeleton can describe a contact quality of backbone aggregates⁴. Further, aggregate skeleton requires a proper packing state of stone and sand particles as backbone aggregates. Vavrik et al. distinguished HMA mixtures into three kinds of aggregate gradation that are stone mastic asphalt (SMA), coarse graded and fine graded⁵. On the other hand, Van de Ven et al. classified HMA aggregate gradation into four skeleton types, namely stone skeleton, stone-sand skeleton, sand-stone skeleton and sand skeleton⁶. However, previous researchers have not properly described gradation structure of those HMA aggregate gradation types.

HMA mixtures comprise high volume fraction of aggregates with asphalt binder filling the gaps between the aggregates. Aggregates mix within HMA is a discrete system. Aggregate particles may interlock each other providing shearing resistance of

sand asphalt mix. When applied shear stress overcomes the shearing resistance, aggregates ride up each other and increase volume of the aggregates mixture. The volume increment or dilatancy properties represent a geometric property of granular mixture governing shear strength. Deshpande and Cebon successfully used single-size sphere assembly model to explain dilatancy behavior of the mixtures⁷. Recently, asphalt researchers reported that real HMA mixtures also showed significant dilatancy⁸. Sphere assembly model appropriately depicted the spatial configuration of aggregate particles within a dense graded HMA mixture⁵. But, multi-sizes sphere assembly models that can describe dilatancy properties of HMA mixtures have not been developed yet. On the other hand, triaxial apparatus, which is expensive and complicated, is currently required to measure dilatancy properties.

The goal of this study was to develop the geometrical models of aggregate gradation structure of HMA. Sphere assembly models were used to describe the geometrical models of HMA aggregate gradation types that are SMA stone skeleton, coarse graded stone-sand skeleton, coarse graded and fine graded sand-stone skeleton. Suitability of the sphere assembly models was examined by comparing dilatancy properties of the sphere assembly models with the ones obtained from the experiment. The

dilatancy properties were obtained from quasi-static compression test, which is quite simpler than triaxial one. Validation on the dilatancy properties was evaluated using graphical and statistical correlation analyses. Shape distortion accompanying with dilatancy phenomenon was considered as permanent deformation. Therefore, dilatancy properties of HMA were compared to dynamic stability (DS) obtained from wheel-tracking test (WTT). Moreover, simple doublet mechanistic was introduced to characterize deformation tendencies of sphere assembly models under WTT.

2. LITERATURE REVIEW

Bailey method simplifies aggregate particles within HMA into four types⁵. These are stone, interceptor, coarse sand and fine sand. Stone and coarse sand particles act as backbone aggregates, which support outer load directly. Stone and coarse sand particles are separated by sieve size 2.36 mm⁶. Fine sands fill in the spaces between stone and coarse sand particles. Interceptors are too large to fit in the voids created by larger coarse aggregate particles. Excessive interceptors and fine sands reduce packing of backbone aggregates. Bailey method categorized HMA mixtures into three kinds of aggregate gradation, namely SMA, coarse graded and fine graded. Bailey method assumes that stone particles act as backbone aggregates on SMA and coarse graded. Meanwhile, coarse sand particles are the backbone aggregates on fine graded. Those HMA aggregate gradation types can be properly designed using the Bailey criteria of CA ratio, FA_c, and FA_f. CA ratio is coarse aggregate ratio. FA_c is fine aggregate coarse ratio. FA_f is fine aggregate fine ratio. The CA ratio criterion facilitates stone particles contacting each other. The FA_c criterion facilitates coarse sand particles tightly packed and fitting the gaps among the stone particles. The FA_f criterion avoids excessive fine sand particles⁵. However, Bailey method did not discuss geometrical models of the HMA aggregate gradation structure types.

Mohr-Coulomb theory states the shear resistance of HMA coming from asphalt mastic cohesion. However, the asphalt mastic cohesion reduces at high temperature. HMA particularly relies on interlocking among aggregate particles to develop the shear strength⁹. Interlocking effect of aggregate particles occurs in a very thin shear band and governs shear strength. Interlocked aggregates permit small shear distortion. During the distortion, aggregate particles in the shear zone ride up each other in a quasi-static motion. Therefore, interlocking on aggregates expresses internal resistance or required work against

shear distortion. On a volume increase during shear distortion, namely dilatancy phenomenon, geometry state of aggregate assembly obviously affects degree of interlocking on aggregate mix. It means that degree of interlocking on aggregate mix can be measured from dilatancy property⁷. Bolton pointed out that dilatancy rate (s) and dilatancy angle (ψ) could express degree of dilatancy¹⁰. s value numerically stays within a range of 0.7 – 1.8. A higher s increases a stiffening effect of confining pressure and reduces shear strain (γ)^{7,9}. γ was considered to be an indicator of plastic deformation for HMA¹¹. **Fig.1** illustrates simplified spheres assembly for aggregate particles and dilatancy phenomenon. When spheres assembly is subjected to shear load, some particles move other particles. The distortion in sphere assembly is represented by ψ and γ properties. s is not an angle, therefore is not described in **Fig.1** with ψ and γ .

A pair of particles (doublet) is considered as a structural unit in a granular medium. The doublet undergoes deformations, i.e. separation, rotation and shearing, when loads are macroscopically applied to the granular medium. Geometrical structure of sphere assembly determines contact angle (θ). The angle affects amount horizontal and vertical components of macro stresses transmitted by the particles. Greater θ increases horizontal macro stress and simultaneously reduces vertical macro stress. **Fig.2** shows microstructure of the doublets and the micro stresses^{12,13}.

A uniform compressive loading on surface of asphalt mixture layer creates a combination of vertical compressive micro stress and horizontal tensile micro stress¹³.

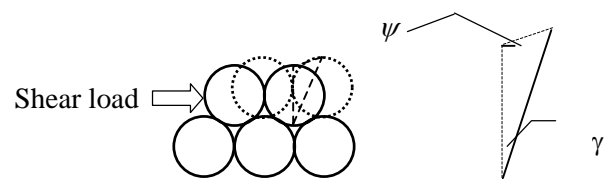


Fig.1 Illustration of dilatancy phenomenon (1986)



Fig.2 Illustrations of microstructure of the doublets and the micro stresses (2005)

3. EXPERIMENTAL WORKS

A goal of the experimental works is to measure dilatancy properties of HMA mixtures. Mix design procedures were carried out to prepare the HMA mixtures specimen for the dilatancy properties measurement.

(1) Preparation of HMA materials and aggregate blend

Mineral aggregates and straight asphalt of Pen 60/80 used in this study are produced in Japan. The relevant Indonesian standards were referred to check suitability of the materials. Coarse and medium aggregates, screening, and coarse and fine sand were involved as mineral aggregates.

Six aggregate gradations were introduced in accordance with each type of aggregate skeletons. Gradations 1, 3, 4, and 6 were designed by combining the Bailey method⁵⁾ and the aggregate skeleton type criteria⁶⁾. The gradation types of the respective Gradations were SMA stone skeleton, coarse graded stone-sand skeleton, coarse graded sand-stone skeleton and fine graded sand-stone skeleton. Two gradations, i.e. Gradations 2 and 5, were arbitrarily selected considering the control points and restricted zone required by the Indonesian standard of HMA. **Fig.3** illustrates the respective gradation curves, and **Table 1** presents the Bailey properties of each gradation. Each reference number of the series is the identical number of aggregate gradation.

Gradation 1 contains high stone fraction (> 75%) and completely follows the Bailey criteria for SMA. Stone skeleton mixes empirically require stone content of not less than 75%¹⁴⁾. Therefore, Gradation 1 is classified as a full SMA stone skeleton.

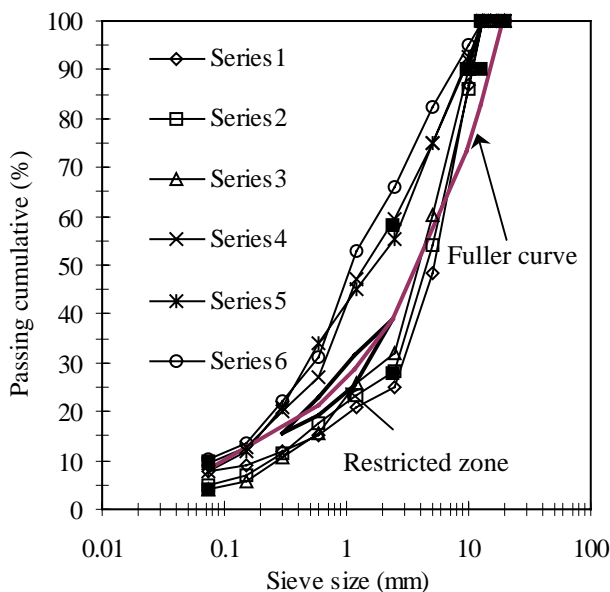


Fig. 3 Aggregate gradations used in this research (2006)

Gradations 2 and 3 contain more stone fraction than sand fraction. But, Gradation 2 partially meets the Bailey criteria for coarse graded, while Gradation 3 fully satisfies the criteria. Therefore, Gradations 2 and 3 are classified as partial and full coarse graded stone-sand skeleton, respectively. Gradations 4, 5 and 6 contain more sand fraction than stone fraction. Gradation 4 fully meets the Bailey criteria for coarse graded, while Gradation 5 partially satisfies the criteria. Therefore, Gradations 4 and 5 are classified as full and partial coarse graded sand-stone skeleton, respectively. Gradation 6 partially satisfies the Bailey criteria for fine graded, so it can be classified as partial fine graded sand-stone skeleton.

(2) Mix design procedure

Refusal density method, which is the current standard protocol of mix design in Indonesia, was used in this study. The mix design procedure was as follows.

1. Prepare aggregates, sand, filler and asphalt.
2. Fabricate Marshall briquettes with six asphalt contents. Every sample was subjected by 75 blows each side.
3. Measure and determine design properties, i.e. volumetric parameters, stability and flow, on each sample.
4. Determine the three asphalt contents to conduct the refusal density compaction. The first asphalt content was initially determined so that the air voids of compacted sample approximately corresponded to 6%. After that, the other asphalt contents were decided as 0.5% lower and 0.5% higher than the first asphalt content. The duplicate specimens were made for each-asphalt content.

Table 1 Bailey properties of the used aggregate gradations (2006)

Grada-tion	Stone Content %	Values of Bailey ratios		
		CA	FA _c	FA _f
1	75.02	0.40 (0.25-0.4) ^a	0.61 (0.6-0.85)	0.61 (0.6-0.85)
2	71.63	0.48 (0.5-0.65)	0.64 (0.35-0.50)	0.38 (0.35-0.50)
3	68.03	0.61 (0.5-0.65)	0.50 (0.35-0.50)	0.36 (0.35-0.50)
4	40.75	0.59 (0.5-0.65)	0.46 (0.35-0.50)	0.47 (0.35-0.50)
5	44.85	0.69 (0.5-0.65) FG CA ^b	0.63 (0.35-0.50) FG FA _c ^b	0.34 (0.35-0.50) FG FA _f ^b
6	34.04	1.67 (0.6-1.0)	0.43 (0.35-0.5)	Not defined

^aNumbers in parentheses are the Bailey criteria, that is suggested values of the Bailey ratios for each HMA type aforementioned in 3(2)⁵⁾. ^bFG CA is CA ratio for fine dense graded mixture, FG FA_c is FA_c ratio for fine dense graded mixture, FG FA_f is FA_f ratio for fine dense graded mixture.

Table 2 Performance requirements of Indonesian wearing course mixture¹⁵⁾ (2002)

The properties of asphalt mixture	Specified values
Voids in mineral aggregates (VMA) (%)	≥ 15
Voids in the mixture (VIM) after 2 × 75 blows (%)	4.9 – 5.9
Voids filled with asphalt (VFA) (%)	≥ 65
VIM at refusal density	≥ 2.5
Stability (kN)	≥ 8
Flow (mm)	≥ 2
Marshall Quotient (kN/mm)	≥ 2
Retained stability index (%)	≥ 85
Asphalt absorption (%)	≤ 1.2

Note: Retained stability index is comparison between the stabilities after the specimens soaked for 24 hours and 30 minutes.

5. Fabricate Marshall specimen according to the refusal density compaction protocol. 400 blows in each side were applied on samples.
6. Determine air void of the samples fabricated by the refusal density compaction.
7. Perform comprehensive evaluation on the asphalt mixture properties to obtain an acceptable range of asphalt content based on the specified requirements as presented in **Table 2**.
8. Determine the optimum asphalt content (OAC), namely the median of satisfactory asphalt contents range obtained from step 7.

(3) Compression test for measuring dilatancy property and specimens preparation

Dilatancy property was measured by compression test. The specimens were fabricated at OAC with the same manner as Marshall specimens. Each specimen had 75 blows on each side. Marshall mold gives the specimen in which size ratio of height to diameter is about 0.6. Erkens¹⁶⁾ carried out the compression test on asphalt mixture specimens with several size ratios. Erkens¹⁶⁾ found that compression test with a low size ratio specimen gave higher values of peak stress and axial strain at peak stress in comparison to the one used the size ratio of 2.0. Therefore, the soap lubricated plastic sheets acting as friction reduction layers were inserted between specimen sides and compression plates. These layers helpfully reduce the discrepancies in peak stress and axial strain at peak stress upon the size ratio of 2.0¹⁶⁾.

The computer-controlled compression test machine recorded the load and displacement during testing. The test was run at a deformation rate of 3.75 mm/minute and a temperature of 30°C. The procedure simulates a reasonably slow loading rate that would be rheologically equivalent to traffic loading associated with rutting¹⁷⁾. The test

temperature was 20°C lower than the average highest pavement temperature in Indonesia, namely 50°C¹⁸⁾. This temperature was also close to the mean monthly pavement temperature of the 27th highly populated cities in Indonesia, that is 31°C¹⁹⁾. Social and economic activities in the cities may generate daily traffic volume, which is critical to rutting.

(4) Data process

Values of γ and s were calculated from final axial-compressive and transversal strains using the following set of equations^{7,20)}.

$$\varepsilon_a = \ln\left(\frac{h_f}{h_0}\right), \quad \varepsilon_t = \ln\left(\frac{D_f}{D_0}\right) \quad (1)$$

$$\varepsilon_v = \varepsilon_a + 2\varepsilon_t \quad (2)$$

$$\gamma = \varepsilon_a - \frac{1}{3}\varepsilon_v \quad (3)$$

$$s = \frac{|\varepsilon_v|}{|\gamma|} \quad (4)$$

Where

$\varepsilon_a, \varepsilon_t, \varepsilon_v$: final axial-compressive, transversal and volumetric strains.

h_0, D_0 : initial height and diameter of specimen (mm).
 h_f, D_f : final height and diameter of specimen (mm).

In this paper, negative sign is used to express axial compressive strain. Positive sign of volumetric strain means increase of volume.

ψ can be measured using triaxial test. During the test, ε_a and ε_t should be recorded, thus $\psi = \tan^{-1}(\dot{\varepsilon}_v/\dot{\gamma})$ can be obtained. However, this study uses sphere assembly model to determine ψ by follows a principle shown in **Fig.1**.

Kendall τ method²¹⁾ was used for correlation analysis on the mixture properties. τ coefficient quantitatively evaluates an agreement between two different measurement systems. The method was used to compare the rankings of the investigated HMA mixtures defined by s, γ and ψ . Sufficient τ values indicates good correlation among those properties. τ is expressed as the following.

$$\tau = \frac{4|L_X \cap L_Y|}{n(n-1)} - 1 \quad (5)$$

Where

L_X, L_Y : set of pairs ranked by X and Y measurement systems, respectively.

$|L_X \cap L_Y|$: the numbers of pairs ranked in the same way by L_X and L_Y .

n : number of observed members.

Table 3 Acceptable asphalt content range and OAC (2006)

Gradation	Range and band of accepted asphalt content (%)	OAC (%)
1	5.25 – 5.42 (0.17)	5.34
2	5.78 – 5.88 (0.10)	5.83
3	5.20 – 5.42 (0.22)	5.31
4	5.20 – 5.63 (0.43)	5.41
5	5.61 – 5.62 (0.01)	5.62
6	5.20 – 5.54 (0.34)	5.37

4. DATA ANALYSIS AND DISCUSSION

(1) The results of mix design

Table 3 presents the acceptable asphalt content range and the OAC. Those results were decided at the final step of the Refusal density procedure as mentioned in Section 3 (2).

The partial coarse graded HMA mixtures, i.e. Gradations 2 and 5, excessively contained interceptors and fine sand particles. For stone particles, the interceptors created additional spaces, which should accommodate asphalt binder and fine sands. Fine sands had a large surface area, which also increased the asphalt binder demand. Improper packing of backbone aggregates within Gradations 2 and 5 inflicted both the mixtures upon a narrow margin of acceptable asphalt content. Gradations 1, 3 and 4 fully satisfied the Bailey criteria. It means that the voids between stone particles were sufficiently filled with coarse sand and fine sand. Therefore, the asphalt binder demand of Gradations 1, 3 and 4 were comparatively lower than that of Gradations 2 and 5. Backbone aggregates within Gradations 1, 3 and 4 were well packed. Thus, Gradations 1, 3 and 4 had a wider margin of the acceptable asphalt content. Gradation 6 particularly comprised the large amount of coarse sand and screening. The coarse sand and screening acted as backbone aggregates within Gradation 6. Stone particles floated within the coarse sand and screening. FG FA_c of Gradation 6 matched with the suggested Bailey ratio for fine graded mixture. It indicated that the coarse sand and screening particles in Gradation 6 were well packed. Consequently, Gradation 6 required lower asphalt binder and had a larger margin of the acceptable asphalt content in comparison to Gradations 2 and 5.

(2) Validation of aggregate gradation models based on dilatancy properties

Table 4 presents s and $|\gamma|$ properties of HMA sample for each Gradation. The range of measured s is 1.03-1.38, which stays within the theoretical values of s as cited in Deshpande et al.'s study⁷⁾. It means that a simple quasi-static compression test is

Table 4 Measured $|\gamma|$ and s (2006)

Gradation	ε_a	ε_t	$ \varepsilon_s $	$ \gamma $	s^a
1	-0.23	0.29	0.35	0.34	1.03
2	-0.21	0.31	0.40	0.35	1.16
3	-0.12	0.19	0.27	0.21	1.29
4	-0.06	0.11	0.16	0.12	1.38
5	-0.08	0.15	0.21	0.16	1.37
6	-0.10	0.17	0.24	0.18	1.34

^a The theoretical values of s are 0.7 – 1.8⁷⁾

suitable to measure a value of s .

Correlation analysis on s and $|\gamma|$ was carried out as follows. Two sets of HMA pairs, namely L_s and $L_{|\gamma|}$, ranked by s and $|\gamma|$ properties were defined. The criteria of which greater s and smaller $|\gamma|$ give better performances were applied. Greater s and smaller $|\gamma|$ indicate a higher interlocking effect on aggregate particles and lower deformation, respectively. Therefore,

$$L_s = \{(2,1), (3,1), (3,2), (4,1), (4,2), (4,3), (4,5), (4,6), (5,1), (5,2), (5,3), (5,6), (6,1), (6,2), (6,3)\}$$

On the member of L_s , (2,1) means that Gradation 2 has better rank than Gradation 1, because s of Gradation 2 is higher than that of Gradation 1. Further,

$$L_{|\gamma|} = \{(1,2), (3,1), (3,2), (4,1), (4,2), (4,3), (4,5), (4,6), (5,1), (5,2), (5,3), (5,6), (6,1), (6,2), (6,3)\}$$

$$L_s \cap L_{|\gamma|} = \{(3,1), (3,2), (4,1), (4,2), (4,3), (4,5), (4,6), (5,1), (5,2), (5,3), (5,6), (6,1), (6,2), (6,3)\}$$

and

$$|L_s \cap L_{|\gamma|}| = 14$$

Using **Eq.(5)**, the coefficient of τ is 0.87. A proper value of τ with a high positive agreement is not less than + 0.60²²⁾. This agrees with soil mechanistic theory, because higher dilatancy property positively reduces shear deformation⁷⁾.

Fig.4 illustrates the various spheres assembly models for describing aggregate gradation structure in this study. Single-size sphere assembly represents SMA stone skeleton (Gradation 1). Coarse graded stone-sand skeleton (Gradation 3) can be described as continuous three-size spheres assembly. The modified densest assembly model with continuous three-size spheres, suggested by Hecht, represents coarse graded sand-stone skeleton (Gradation 4)²³⁾. Gradation 4 contains more sand particles than Gradation 3. The model of Gradation 4 involves the layers of coarse and fine sand particles, which separate stone particles mutually. These layers can hold more sand particles. Fine graded sand-stone skeleton (Gradation 6) can be modeled as cubical spheres assembly. The cubical spheres assembly allows fine sand particles to occupy the space between coarse sand particles.

Gradations 2 and 5 may contain interceptors

occupying the spaces between stone particles. The interceptors clearly create additional voids and reduce the densest packing of backbone aggregates both in the stone-sand skeleton and stone-sand skeleton. The interceptors spread out the stone particles thus enlarge θ . **Fig.4(b)** and **Fig.4(e)** show the models containing the interceptor. Following Bailey method⁵, stone particles act backbone aggregates in SMA stone skeleton and coarse graded, while coarse sand particles do backbone aggregates in fine graded. Motions of stone or sand particle characterize the dilatancy properties on Gradations 1 to 5 and Gradation 6. The respective motions are also illustrated in **Fig.4**. Each triangle shows the motion of stone with ψ and γ , which express shear distortion due to shear action.

Fig.5 depicts both of ψ and γ more clearly. From comparisons of backbone aggregate motions based on the spheres assembly models, the tendencies in ψ and γ are summarized as follows.

1. ψ on Gradation 4 \approx ψ on Gradation 5 $>$ ψ on Gradation 3 $>$ ψ on Gradation 6 \approx ψ on Gradation 2 $>$ ψ on Gradation 1.
2. γ on Gradation 4 \approx γ on Gradation 6 $<$ γ on Gradation 5 $<$ γ on Gradation 3 $<$ γ on Gradation 1 $<$ γ on Gradation 2.

Kendall τ method also was carried out to further investigate the correlations between the tendencies

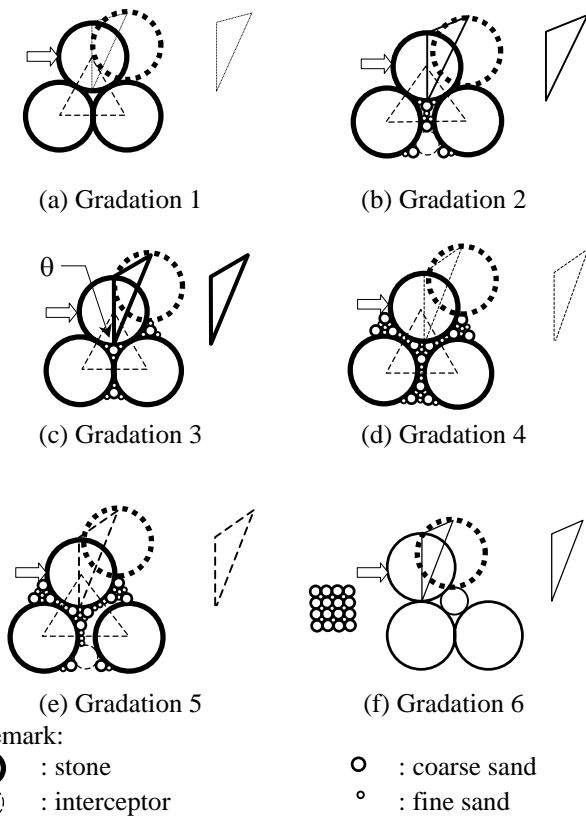


Fig. 4 Sphere assembly models (2006)

in ψ and s shown in **Table 4**. The analysis gets $|L_{\psi} \cap L_s| = 12$ that are $\{(2,1), (3,1), (3,2), (4,1), (4,2), (4,3), (4,6), (5,1), (5,2), (5,3), (5,6), (6,1)\}$. Using **Eq.(5)**, τ value for the correlation between ψ and s was $+0.60$. On the other hand, there were 13 number of pairs ranked in the same way by modeled and measured γ , including $\{(1,2), (3,1), (3,2), (4,1), (4,2), (4,3), (4,5), (5,1), (5,2), (5,3), (6,1), (6,2), (6,3)\}$. So, τ was $+0.73$. Both the tendencies of ψ and γ on spheres assembly models are appropriate to measured s and γ . Consequently, it can be verified that the proposed spheres assembly models using dilatancy properties are effective to evaluate an aggregate gradation structure in HMA. From the illustration, γ of Gradations 2 and 5 were greater than that of Gradations 3 and 4 respectively. It may indicate that reduction of the densest packing of backbone aggregates increased γ of HMA mixtures.

(3) Evaluation of HMA using wheel-tracking test

Rutting potential for all of the mixtures discussed in this study were evaluated using WTT. The test was conducted at a temperature of 60°C , a wheel speed of 42 pass/min, and a load of 686 N. DS, in cycles/mm, has been derived as the indicator of rutting potential. **Table 5** shows θ (in degree) and the results of WTT along with $|\gamma|$ and s .

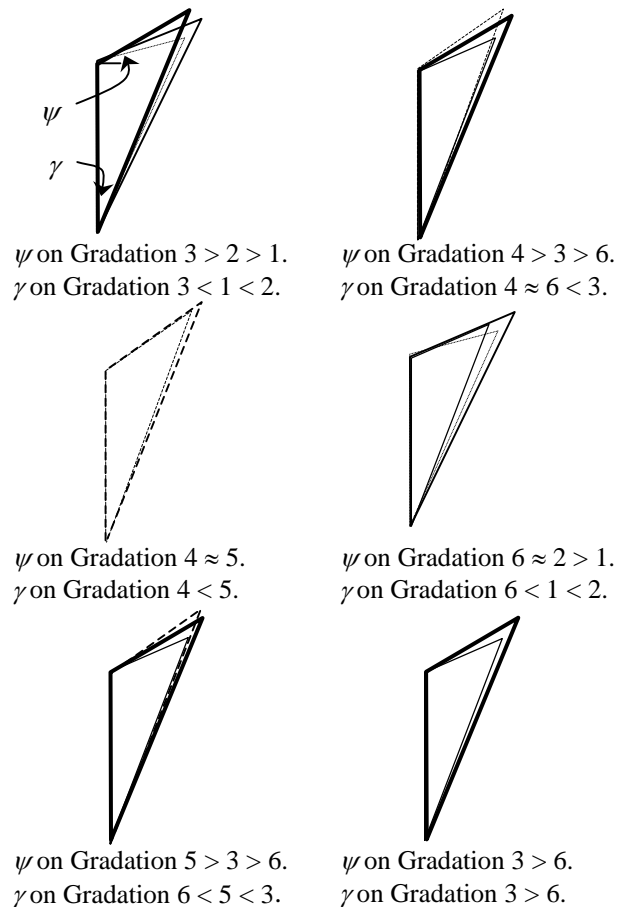


Fig. 5 Comparison of ψ and γ properties (2006)

Table 5 θ , DS, $|\gamma|$ and s for respective Gradation samples (2006)

Grada- tion	1	2	3	4	5	6
θ^a	60	> 60	60	60	> 60	0
DS	759	505	676	993	790	1,116
$ \gamma $	0.34	0.35	0.21	0.16	0.16	0.18
s	1.03	1.16	1.29	1.38	1.37	1.34

^a θ should be considered as approximation values rather the exact ones.

Correlations between $|\gamma|$ and DS, and between s and DS were discussed. Based on **Table 5**, τ for γ and s were + 0.60 and + 0.47 respectively. Following Bhasin et al.s' criterion²²⁾, γ adequately correlates with DS because both properties have τ not less than + 0.60. However s insufficiently correlates with DS. Consequently, s is not a good indicator for rutting assessment. Greater s may indicate better rutting resistance as shown in coarse graded stone-sand skeleton (Gradations 2 and 3). However, s poorly indicate the rutting resistance of Gradation 4 and Gradation 5. Also, s obviously underestimates the rutting resistance of Gradation 1 and Gradation 6. The correlations between $|\gamma|$, s and DS are not high because compaction procedures of Marshall tamping and wheel tracking roller may appear differences within internal structure of the Marshall and WTT specimens. Also, this dilatancy theory stands on an assumption that stone and sand particles are sphere balls. However, real stone, sand and screening particles don't always fit to the assumption.

Doublet mechanistics can predict the surface loading, which induces compressive and tensile stresses in the region below the loading surface. The stress state of HMA in WTT is quite different from that in dilatancy phenomena caused by shear action. Under WTT, the backbone aggregates of HMA do not develop dilatancy as a response from the loading stresses. Tensile stress separates lower spheres from the group. When the lower spheres spread out, support on upper sphere reduces. As a result, the spheres group undergoes consolidation, which appeared as rutting. Interceptors enlarges θ and increases tensile stress component. Increase of tensile stress spread out the lower sphere group wider and consolidates the group of spheres deeper.

Small θ limits tensile stress. Small tensile stress reduces separation and restricts consolidation. **Fig.4** shows that θ of Gradation 1 \approx 3 < θ of Gradation 2, while θ of Gradation 5 > θ of Gradation 4. It can be seen that Gradations 2 extensively experienced rutting rather than Gradations 1 and 3. Further, rutting of Gradation 5 is greater than that of Gradation 4. Kondo et al.²⁴⁾ observed that stone

particles in a slab HMA specimen underwent rotation during WTT. The rotation does not spread out the lower spheres group. Thus, contribution of the rotation on rutting progression is less significant than the one by the separation. Gradation 1 contains about 75 % of stone content which is more than that of Gradation 3. Considering the stone content, the rotation of stone particles in Gradation 1 could be extensive than that in Gradation 3. However, the sphere assembly models can not distinguish the rotation and separation of stone particles in both gradations. Consequently, the sphere assembly models can't explain why Gradation 1 has higher DS than Gradation 3, despite θ of both gradations is almost same. Readers also can ask why DS value of the coarse graded sand-stone skeleton (Gradations 4 and 5) is greater than that of SMA stone skeleton (Gradation 1). The sand-stone skeleton comprises high sand content that effectively adheres asphalt together. The adhesion between coarse sand particles and asphalt enhances bonding strength of asphalt mastic. Viscosity of the asphalt mastic is consequently improved, and the asphalt mastic develops considerable HMA cohesion. At the high temperature, a part of the cohesion of Gradations 4 and 5 is probably still left for resisting rutting. **Fig.4** also shows that cubical structure of Gradation 6 having $\theta = 0$, which strictly avoids tensile stress. Gradation 6 contains about 66 % sand fraction. The high sand content in Gradation 6 effectively improve the mix cohesion even at the WTT temperature. As the result, Gradation 6 has the highest DS.

5. SUMMARY

The conclusions of this study are summarized as follows.

1. A simple compression test is reliable to determine shear strength properties of s and γ .
2. Multi-size spheres assembly models of aggregate gradation structure are developed for SMA stone skeleton, coarse graded stone-sand skeleton, coarse graded sand-stone skeleton and partial fine graded sand-stone skeleton. The tendency of dilatancy property obtained by the sphere assembly model sufficiently agrees with the one measured by compression test. Thus, the proposed spheres assembly models using dilatancy properties are effective to evaluate an aggregate gradation structure in HMA.
3. s cannot completely represent rutting resistance, DS. Greater s adequately indicates better rutting resistance for coarse graded stone-sand skeleton and coarse graded sand-stone skeleton types. However, s obviously underestimates rutting

resistance of SMA stone skeleton, and fine graded sand-stone skeleton type.

4. The doublet mechanics can qualitatively describe deformation tendencies on the sphere assembly models of HMA under WTT by taking separation, rotation, and consolidation of particles into account. Small θ and high mix cohesion positively increase rutting resistance.

REFERENCES

- 1) Kandhal, P.S. and Mallick, R.B : Effect of mix gradation on rutting potential of dense graded Asphalt mixtures, *TRB No. 1767, Asphalt Mixtures*, pp. 146-151, 2001.
- 2) Abdullah W.S., Obaidat, M.T. and Abu-Sa'da N.M : Influence aggregate type and gradation on voids of asphalt concrete pavements, *ASCE Journal of Materials, Civil Engineering*, 10(2), pp. 76-85, 1998.
- 3) Ruth, B.E., Roque, R. and Nukunya, B : Aggregate gradation characterization factors and their relationship to fracture energy and failure strain of asphalt mixtures, *Journal of AAPT*, Vol. 71, pp. 310-331, 2002.
- 4) Katman, H.T., Karim, M.R., Ibrahim, M.R. and Mahrez, A : Effect of mixing type on perf. of rubberised porous asphalt. *Proc. of the EASTS*. Vol. 5, pp. 762-771, 2005.
- 5) Vavrik, W.R., Huber, G., Pine, J.W., Carpenter S.H., and Bailey R. *TR Circular, No. E-C044: Bailey method for gradation selection in HMA mixture design*. Washington D.C, October 2002.
- 6) Van de Ven, M.F.C., Voskuilen, J.L.M. and Tolman, F. : *The spatial approach of hot mix asphalt*. 6th RILEM Symposium PTBEM'03, Zurich, Switzerland, 2003.
- 7) Deshpande, V.S. and Cebon, D. : Steady-state constitutive relationship for idealised asphalt mixes. *Mech. of Mat.* 31, pp. 271-287, 1999.
- 8) Ossa, E.A., Taherkhani, H. and Collop, A.C. : *Compressive deformation behavior of asphalt mixtures* (Abstract). *J. of AAPT 2006* (online at <http://www.asphalttechnology.org>).
- 9) Pellinen, T.K. and Song J. Xiao, S. : *Characterization of hot mix asphalt with varying air voids content using triaxial shear strength tes*, September 2004, <http://asac.csir.co.za>.
- 10) Bolton, M.D. : The strength and dilatancy of sands. *Geotechnique* 36, No.1, pp. 65-78, 1986.
- 11) Von Quintus, H.L., Scherocman, J.A., Hughes, C.S. and Kennedy, T.W. *NCHRP Report 338: Asphalt-aggregate mixture analysis system AAMAS*, TRB, March 1991.
- Washington, D.C.
- 12) Zhang, Q. and Britton, M.G. : A micromechanics model for predicting dynamic loads during discharge in bulk solids storage structures. *Can. Biosystem Eng.* 45, pp 5.21-5.27, 2003.
- 13) Sadd, M.A. and Dai, Q. : A comparison of micro-mechanical modeling of asphalt materials using finite elements and doublet mechanics. *Mech. Of Mat.* 37, pp. 641-662, 2005.
- 14) Sluer, B.W., Wanders, G.W.J., Smith, H.J.J. and Gouw, S. : Crushed stone skeleton mixes in interlayer a weapon in the battle against rutting?, *2nd Eurasphalt and Eurobitume Congress*. Barcelona, pp. 530-538, 2000.
- 15) Directorate General of Highway - Republic of Indonesia. *Indonesian national standard: specification of hot mixed asphalt*. Indonesia, 2002.
- 16) Erkens, S.M.J.G. : *Asphalt concrete response (ACRe): determination, modeling and prediction*. PhD Dissertation. Technical University Delft. Netherlands. 2002.
- 17) Christensen, D.W., Bonaquist R., Anderson, D.A. and Gokhale, S. : Indirect tension strength as a simple performance test, *TR Circular No. E-C068: New Simple Performance Tests for Asphalt Mixes*, pp. 44-57, 2004.
- 18) Soedjatmiko E. A. T. : *Characterization of asphalt layer modulus for Indonesian temperature condition*, MSc. Thesis, Institute Technology Bandung, Indonesia, 1999.
- 19) Tjan, A. and Ignatius, W. : *Rut depth prediction based on viscoelastic prediction*, Paper presented in 2nd Asia Pacific Conf. & Exhibit on Trans. Environ. Beijing, China, 2000.
- 20) Selvakumar, R. and Narayanasamy, R. : Deformation behavior of cold upset forming of sintered Al-Fe composite preforms, *J. Eng. Mat. Tech.*, Vol. 127, pp. 251-256, 2005.
- 21) Denoux, T. Mason, M.H. and Hebert, P.A. : Non-parametric rank-based statistics and significance test for fuzzy data. *Fuzzy Sets and Systems* 153 1-28, 2005.
- 22) Bhasin, A. Button, J.W. and Chowdhury, A. : *Evaluation of selected laboratory procedures and development of databases of HMA* Report No. FHWA/TX-05/0-4203-3TTI, Texas A&M Univ. System College, 2005.
- 23) Hecht, C.A. : Geomechanical models for clastic grain packing, *Pure and Applied Geophysics* 161, pp. 331-349, 2004, <http://www.springerlink.com>.
- 24) Kondo, T., Moriyoshi, A., Yoshida, T., and Takahashi, S. : Crack formation in asphalt mixtures in the wheel tracking test at high temperature, *J. of the Japan Petroleum Inst.*, 47(2), pp. 90-99, 2004.

ダイレイタンシー特性に基づいたわだち掘れ評価の骨材粒度モデル

Iman HARYANTO・高橋 修

アスファルトコンクリート（アスコン）のせん断変形抵抗性は骨材粒度に依存している。アスコンにおける骨材粒子の位置関係は円形粒子の集合体でモデル化されるが、本研究では、アスコンの骨材粒度を SMA 骨子モデル、粗粒 stone-sand 骨子モデル、粗粒 sand-stone 骨子モデル、細粒 sand-stone 骨子モデルの 4 タイプに分類して、それぞれの円形粒子集合体モデルを提案した。これらの骨材粒度モデルに対するダイレイタンシー特性値を比較することにより、アスコンのわだち掘れ評価が可能であることを示した。各骨材粒度モデルが実際のアスファルト混合物に対して妥当であること、およびダイレイタンシー特性値がわだち掘れ評価に有効であることは一軸圧縮試験とホイールトラッキング試験を実施して確認した。